Causes and Prevention of Splitting/Bursting Failure of Concrete Crossties: A Computational Study

Hailing Yu
Structures and Dynamics Division
Volpe National Transportation Systems Center
55 Broadway, Cambridge, MA 02142 USA
Email: hailing.yu@dot.gov
Phone: (617) 494-2554

4229 words, 1 table (250 words), 12 figures (3000 words) = 7479 words

ABSTRACT

Concrete splitting/bursting is a well-known failure mode of concrete crossties that can compromise the crosstie integrity and raise railroad maintenance and track safety concerns. This paper presents a computational study aimed at better understanding the main contributing factors to this failure mode. Finite element models are developed for concrete crossties with different geometric and reinforcement configurations. The investigated factors include: steel reinforcement type, concrete release strength, presence of fastener shoulders, and cyclic dynamic loading. Five steel reinforcements with various surface geometries, including a smooth wire, three indented wires and a seven-wire strand, are studied. Three concrete release strengths are applied at 3,500, 4,500 and 6,000 psi, respectively. Static analyses of pretension release and dynamic analyses of repeated rail seat loading are conducted. The study concludes that low concrete release strengths, accompanied by underdeveloped steel-concrete bond for prestress transfer, are responsible for initial concrete material degradation patterns that can further deteriorate under cyclic dynamic loading and develop into macroscopic cracks consistent with the field observations. Based on these findings, this paper recommends (1) sufficiently high concrete release strengths during production and (2) development and implementation of a qualification test standard with dynamic loading cycles to ensure long term splitting/bursting performances of concrete crossties.

INTRODUCTION

Concrete ties were considered a promising alternative to traditional timber ties with their many perceived advantages. However, since their first major installation in North America in 1966 (*1*), prestressed concrete ties have displayed several failure modes in the field that have led to the premature replacement of track components and sometimes derailment accidents (*2*). These failures have prevented more widespread use of the concrete ties.

Figure 1 shows two examples of the bursting or splitting failure mode. The concrete crosstie on the left had twenty prestressing wires, and multiple bursting cracks were observed originating and branching out from the steel-concrete interfaces, coalescing and even developing into horizontal and vertical cracks along the length of the tie (*3*). The crosstie on the right was made with eight prestressing strands arranged in two rows, and it was split with a horizontal crack in the plane across the top row strands, in a well-known case of widespread horizontal cracks leading to a large scale replacement of the pre-2003 concrete ties on the Amtrak's Northeast Corridor (*4*). The bursting or splitting cracks are detrimental to the structural integrity of concrete crossties and raise both railroad maintenance and track safety concerns. These cracks are generally attributed to the splitting forces transmitted from the prestressing wires or strands to the surrounding concrete, but the exact contributing factors and conditions remain poorly understood. This has impeded the industry's effort to develop effective preventative measures.

Figure 1. Examples of concrete crosstie bursting (left, *3*) and splitting failures (right, *4*).

Concrete crossties are made by embedding prestressed steel reinforcements in concrete and releasing the pretension in the reinforcements once the desired concrete strength is achieved. Releasing the pretension leads to enlarged diameters of the steel reinforcements and hence dilated steel-concrete interfaces owing to the Hoyer effect. Further, natural or manufactured surface geometries on steel reinforcements can produce additional interface dilatations that transmit greater splitting forces. To characterize these interface bond-slip and dilatational mechanisms, macroscale elastoplastic finite element (FE) bond models were developed for various reinforcement interfaces, including those of a smooth wire, a seven-wire strand and three indented wires (*5-7*). Most recently, unified elastoplastic formulations were developed and implemented to characterize the bond behavior of the diversity of reinforcements described above using one bond model (*8*). Both the reinforcement surface geometry and the concrete properties such as release strength can significantly affect the bond behavior in a steel-concrete interface.

This paper applies the FE analysis (FEA) method to study the causes of the bursting/splitting failures of concrete crossties. The FEA framework incorporates the damaged plasticity modeling of concrete, the unified interface bond model referenced above, and modeling of the ballast and subgrade support. This enables the investigation in this paper of four potential contributing factors/conditions: reinforcement surface geometry, concrete release strength, presence of fastener shoulders and cyclic dynamic loads. The simulation results are then presented, based on which recommendations are made on preventing the splitting/bursting failures from occurring in pretensioned concrete ties.

FINITE ELEMENT ANALYSIS FRAMEWORK
This section describes the various modeling components included in the FEA framework as well as some limitations of the modeling approach. The commercial FEA software Abaqus was employed (*9*).

Prestressing Wire/Strand Configuration
Two concrete crosstie designs, similar or equivalent to the two ties shown in Figure 1, were considered in this paper. The first tie has twenty prestressing wires, each with a nominal diameter of 0.209 in. (5.32 mm) and a nominal initial tensile stress of 203 ksi (1,399.6 MPa). Four surface geometry types were considered for these wires: one smooth, one with spiral indentations and two with chevron indentations. These wire surface types were labeled WA, WE, WG and WH, respectively, consistent with the labeling system employed in the Kansas State University's (KSU) bond testing and transfer length measurement studies on the commercially available prestressing wires and strands (*10-13*).

The second tie has eight seven-wire strands arranged in two rows, and the nominal initial tensile stress is 156 ksi (1,075.6 MPa). The steel strands have a nominal diameter of 3/8 in. (9.525 mm) and a yield strength of 270,600 psi (1,865.7 MPa). The strands have natural spiral surfaces and correspond to the strand type SA in the KSU studies.

Concrete Material Modeling
A damaged plasticity model was applied in the material modeling of the concrete. The model uses isotropic damaged elasticity in combination with isotropic tensile and compressive plasticity to represent the inelastic behavior of concrete (*9*). Tensile and compressive damages in concrete are characterized as strength degradations and represented by tensile and compressive damage variables, respectively. As indicated by the uniaxial tensile stress-strain curve in Figure 2, the tensile damage variable d_t measures the degree of tensile strength degradation in the post peak portion of the curve, where d_t=0 indicates undamaged concrete, and d_t=1 indicates completely degraded tensile strength and formation of macro-cracks.
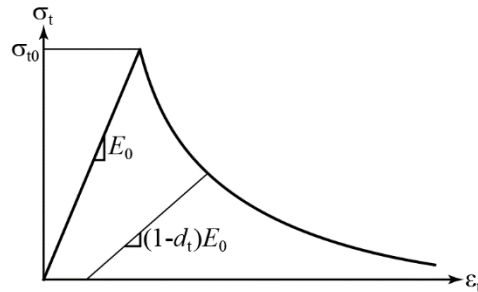
Figure 2. Concrete stress-strain (σ_t-ε_t) curve under uniaxial tension, and definition of the tensile damage variable d_t.

The constitutive equations and material parameters needed to apply this model were described in previous publications (*14-15*). Consistent with the KSU studies, three nominal release strengths were considered: 3,500, 4,500 and 6,000 psi (24.1, 31.0 and 41.4 MPa) (*11*). The basic concrete material properties corresponding to these three release strengths, including elastic modulus, split tensile strength and compressive strength, are summarized in Table 1 and were applied in the simulations presented in this paper.

Table 1. Concrete material properties.

Nominal release strength	3500 psi	4500 psi	6000 psi
Elastic modulus	3,259 ksi (22.5 GPa)	3,655 ksi (25.2 GPa)	4,028 ksi (27.8 GPa)
Split tensile strength	366.0 psi (2.52 MPa)	439.4 psi (3.03 MPa)	478.8 psi (3.3 MPa)
Compressive strength	3586.0 psi (24.7 MPa)	4570.2 psi (31.5 MPa)	5977.8 psi (41.2 MPa)

Bond Modeling
The KSU studies indicated a wide range of bond behaviors resulting from the different reinforcement surface geometries (*16*). The unified elastoplastic bond model (*8*) was applied in this study to simulate the different interface behaviors, with a different set of bond model parameters determined for each reinforcement type. The bond model parameters corresponding to the 6,000 psi (41.4 MPa) concrete release strength were calibrated using both untensioned pullout and pretensioned prism test data generated in the KSU project. However, a simplified calibration method using only the pretensioned prism test data was adopted for the lower concrete release strengths, as untensioned pullout test data were unavailable at the 3,500 and 4,500 psi (24.1 and 31.0 MPa) release strength levels.

The bond model parameters can be roughly categorized in two groups: bond strength related and dilatation related. It was generally assumed that the bond was less developed at lower concrete

release strengths resulting in lower bond strength related parameters, but that the dilatation related parameters remained the same due to similar interface sliding mechanisms. In the particular case with the wire type WH, however, the dilatational rate was assumed to decrease with increased concrete release strengths; this was based on the assumption that owing to the particular WH surface indentations, there would be less sliding but more crushing in the interfaces under higher concrete strengths, as the stronger and stiffer concrete would conceivably place more confinement on the interfacial displacements.

Ballast and Subgrade Modeling

The Extended Drucker-Prager plasticity model was applied to the ballast material. The ballast model was assigned homogeneous material properties and supported by an elastic subgrade, which was modelled as a 30x600x500 in^3 (762x15,240x12,700 mm^3) rectangular box. The ballast and subgrade were modelled for a width equal to one tie spacing. The tie spacing and ballast depth were assumed to be 30 in. (762 mm) and 24 in. (609.6 mm), respectively. The ballast was assigned an elastic modulus of 30,168 psi (208 MPa) and a yield strength of 58 psi (0.4 MPa). The subgrade was assigned an elastic modulus of 72,519 psi (500 MPa). The concrete crosstie-ballast and ballast-subgrade interactions were modelled using contact definitions with a coefficient of friction of 0.5. Figure 3 shows the schematic of a quarter symmetric crosstie-ballast-subgrade model.
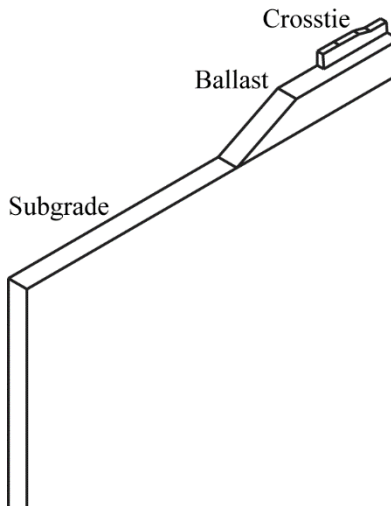
Figure 3. Schematic of a quarter symmetric crosstie-ballast-subgrade model (only partial of the subgrade model is shown in the vertical depth dimension).

Inclusion of Fastener Shoulders

The effect of the fastener shoulders embedded in the concrete crossties was also studied in the FEA. There are many designs of the fastener shoulders, and their complex geometries, if imported exactly into the FEA, can introduce tremendous computational difficulties in terms of mesh quality and numerical accuracy. To avoid such difficulties while still achieving a good understanding on how the presence of fastener shoulders may affect the initiation and growth of the splitting/bursting cracks, simplified FE models of the fastener shoulders were developed following the basic dimensions but omitting the many intricacies of the actual geometries. Figure 4 shows cross sections of the simplified fastener shoulder models embedded within the 8-strand and 20-wire concrete ties, respectively. The 8-strand tie was modeled after the pre-2003 Northeast Corridor concrete ties. The fastener shoulders in these ties were deeply embedded reaching between the upper and lower rows of strands. The fastener shoulders modeled for the 20-wire tie had greatly simplified geometries but retained the main feature of twin stems reaching into the first row of the wires. The fastener shoulders were assigned elastic cast iron properties with an elastic modulus of 18,129,717 psi (125 GPa) and a Poisson's ratio of 0.25.
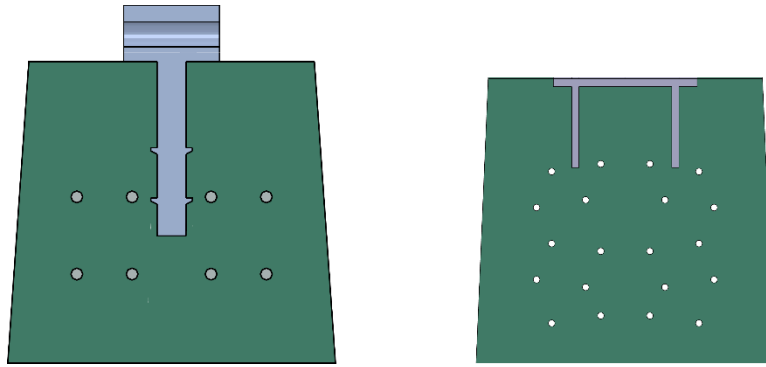
Figure 4. Simplified modeling of fastener shoulder embedment in the 8-strand (left) and 20-wire concrete crossties (right). The cross sections are shown near the rail seats.

Static and Dynamic Analyses

Concrete crossties are pretensioned concrete members that come with initial stress states as a result of the pretension release or prestress transfer phase during production. The pretension release phase was simulated by initially assigning a tension of 156 ksi (1,075.6 MPa) for each strand and 203 ksi (1,399.6 MPa) for each wire. The initial tension was then released in static analyses resulting in prestress transferred stress states, which were then applied as initial conditions in the subsequent dynamic FE analyses.

The dynamic FE analyses simulated the responses of the concrete ties in a rail seat positive bending mode with the type of ballast and subgrade support described in "Ballast and Subgrade Modeling." The concrete ties were subjected to dynamic rail seat loading either through distributed traction loads over the rail seat or a point load on the rail when the fastener-rail assembly was included. The resultant rail seat load was set at 62.1 kips (276.2 kN), which was calculated based on an axel load of 82 kips (364.8 kN), a load distribution factor of 0.505 and an impact factor of 200% (*17*). Under the assumptions that a railcar passes four tie spacing in the duration of a dynamic load and that each tie spacing ranges from 20-30 in. (508-762 mm) in length, the dynamic load duration was calculated to vary from 0.075-0.11 seconds for a railcar traveling at 60 mph (96.56 km/h). The dynamic load duration in the simulations was selected to be 0.1 seconds. Because the dynamic load with this duration did not produce any impact effect in the simulations, the inclusion of the impact factor in calculating the dynamic load appeared necessary. This paper did not explore the possibility of achieving the impact effect by varying the duration of the dynamic load.

Figure 5 defines one loading cycle that lasts 0.1 seconds, with the rail seat force increasing linearly from 0 to 62.1 kips (276.2 kN) in the first 0.05 seconds and then deceasing linearly to 0 in the second 0.05 seconds. Owing to the time consuming nature of the dynamic FEA, only three repeated dynamic load cycles were simulated for each scenario under study.
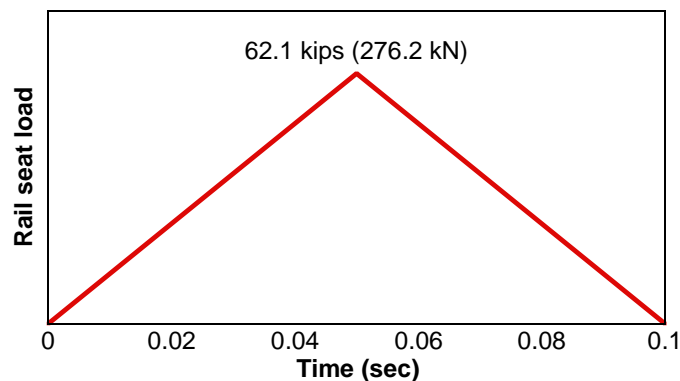
Figure 5. Definition of one dynamic loading cycle.

Limitations

It is well known that concrete material properties evolve over time. Ideally while the static FEA of the prestress transfer process assumes short term concrete properties (i.e., at release), the dynamic FEA should assume longer term concrete material properties featuring higher elastic moduli, tensile strengths and compressive strengths. However, owing to the inflexibility in the FEA program to change material properties between continued analyses, the FEA conducted in this paper assumed the same concrete material properties at release for both short and longer term behaviors. Secondly, as discussed in "Bond Modeling", the bond model parameters corresponding to the two lower concrete release strengths were calibrated using a simplified method with limited available test data. Finally, the effects of concrete creep, concrete shrinkage and steel relaxation that can lead to prestress losses were not considered.

RESULTS

For both the static analyses (of prestress transfer) and the dynamic analyses (of rail seat positive bending), a key outcome examined was the tensile damage profile of concrete indicated by the tensile damage variable d_t (see "Concrete Material Modeling"). In this study, the d_t contour for elements satisfying $d_t \geq 0.05$ after pretension release was plotted for each simulated scenario. On this contour, the maximum d_t ($d_{t,max}$) was of great interest, because d_t approaching 1 would indicate potential cracking. In addition, the extent of damage in the length direction (L_{dt}, the maximum element-to-element distance measured on the contour in the tie's length direction) was calculated to assess the spatial extent of the concrete damage. The dependence of the $d_{t,max}$ and L_{dt} characteristics on reinforcement types and concrete release strengths was first examined. The evolution of the tensile damage profile after experiencing dynamic loading cycles was further evaluated for their potential to develop into macro-cracks. It was noted that the dynamic loading sometimes introduced small scale concrete damages in the concrete-ballast interfaces, but they were not included in the calculations of $d_{t,max}$ and L_{dt} owing to their irrelevance to bursting/splitting damages. These results were presented without and then with the inclusion of the simplified fastener shoulder models.

Without Fastener Shoulders

Figure 6 shows the d_t contours for elements satisfying $d_t \geq 0.05$ upon pretension release for the four prestressing wire geometries at the three concrete release strengths. Figure 7 shows the same contours for the prestressing strand. A quarter of an actual tie was modeled due to symmetries about the center cross sectional and longitudinal planes. The symmetric cross-sectional contours were mirrored to show the full cross-sectional views in these figures.

Figure 6 indicates that the tensile damage profiles are minimal for WA and WE at all concrete release strengths and for WG and WH at the two higher release strengths. On the other hand, the contours in Figure 7 show more significant tensile damages with the prestressing strand; particularly at the 3,500 psi (24.1 MPa) release strength, the damages interconnected in both the upper and lower strand planes in a similar "horizontal" pattern observed in the field (Figure 1, right), even though the horizontal cracks observed in the field were limited to occur in the concrete tie's upper strand plane only.
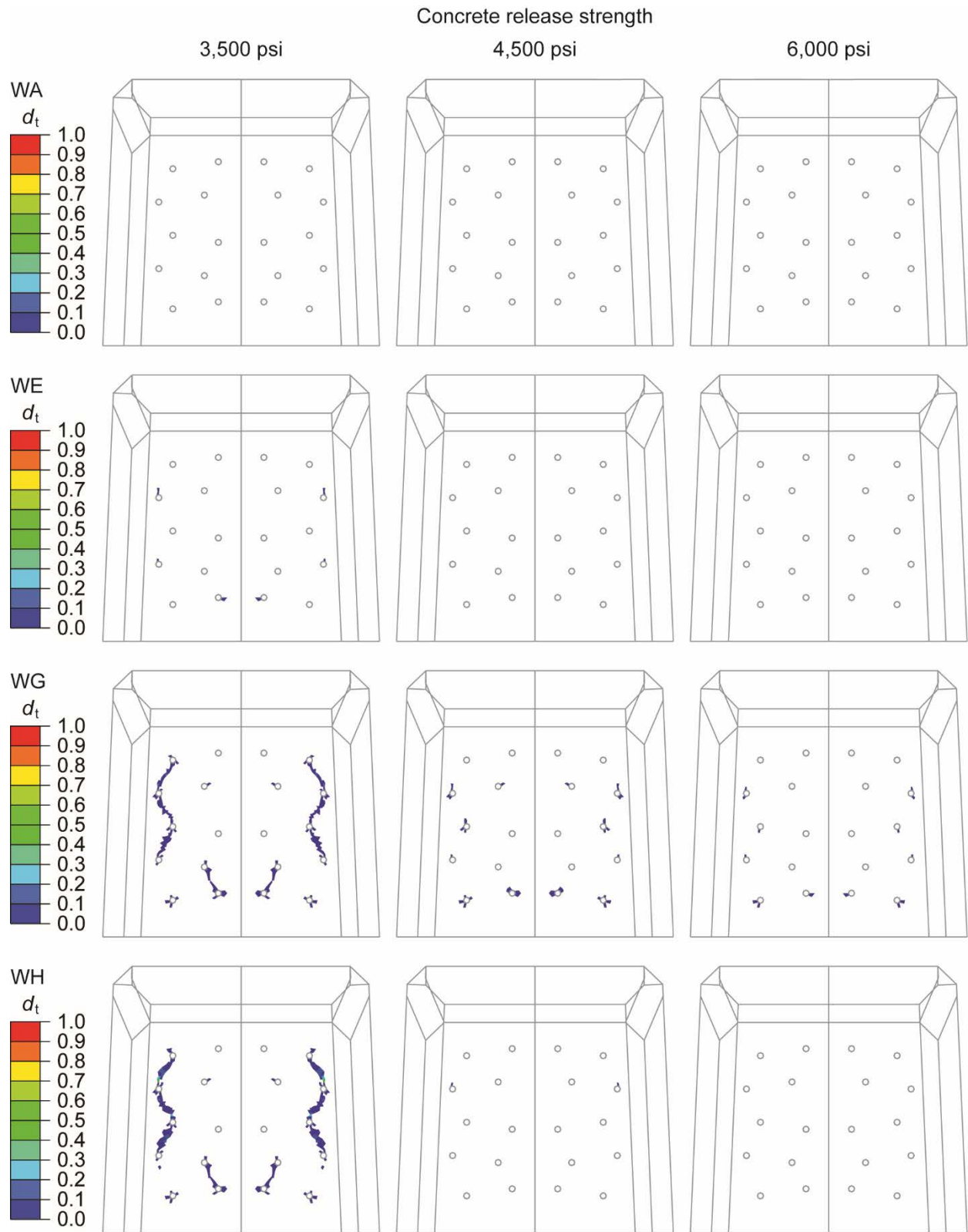
Figure 6. Tensile damage profiles ($d_t \geq 0.05$) after pretension release with four surface geometries and at three concrete release strengths for the prestressing wires.

Concrete release strength

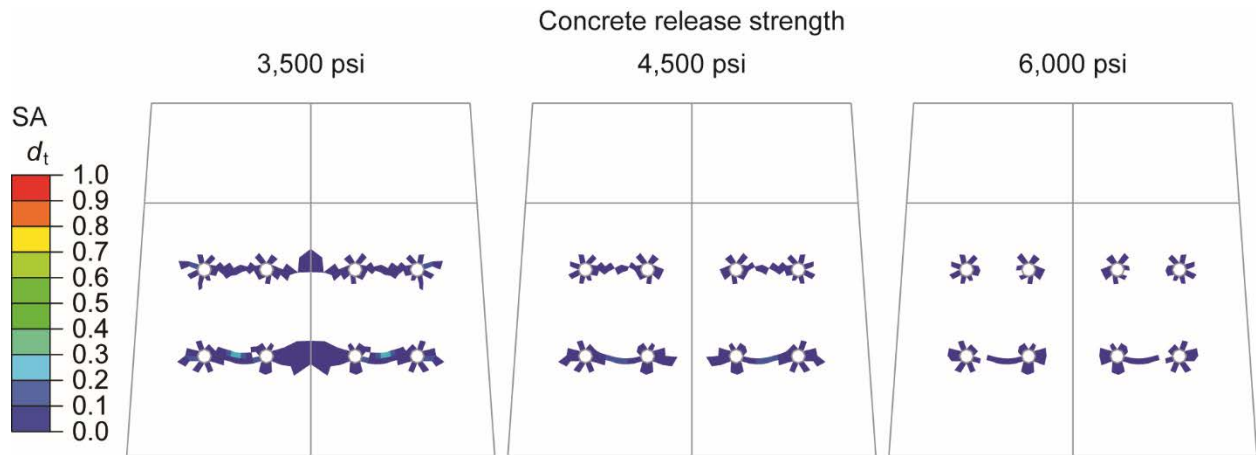3,500 psi   4,500 psi   6,000 psi

Figure 7. Tensile damage profiles ($d_t \geq 0.05$) after pretension release at three concrete release strengths for the prestressing strand.

Each static simulation of pretension release was continued for three cycles of dynamic FEA under the loading depicted in Figure 5. Figure 8 shows the evolution of $d_{t,max}$ and L_{dt} from static to dynamic simulations with the four prestressing wires at the 3,500 psi (24.1 MPa) release strength, and Figure 9 shows the $d_{t,max}$ and L_{dt} evolution with the prestressing strand at all three concrete release strengths. Dynamic loading appeared to increase both damage measures at the lower release strengths. It is noted that L_{dt} may be overestimated because of the continued use of concrete release properties as opposed to longer term properties during the dynamic loading cycles, but the prediction of the increased potential to crack ($d_{t,max}$) was more reasonable because the initial damages presented irreversibly weakened spots in the concrete, and the dynamic loading appeared to have an effect of further weakening the initially damaged materials.
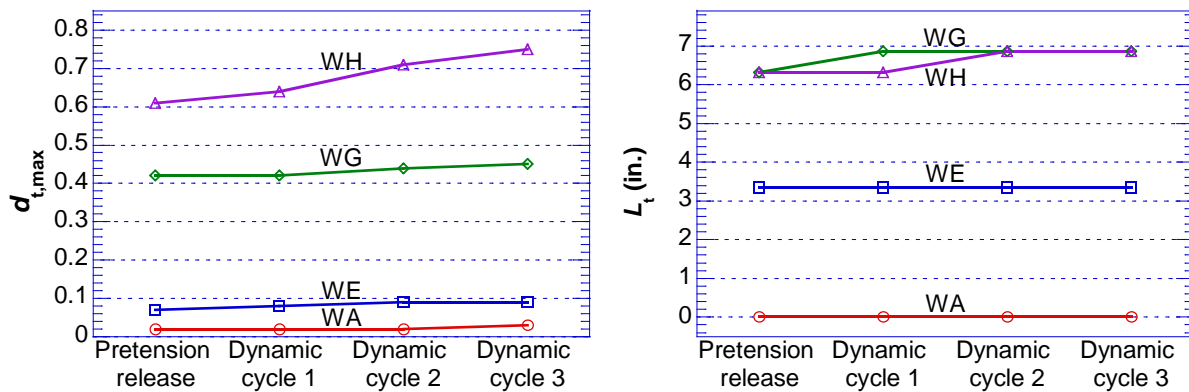
Figure 8. Evolution of $d_{t,max}$ and L_{dt} from static to dynamic simulations with the four prestressing wires at the 3,500 psi (24.1 MPa) concrete release strength.
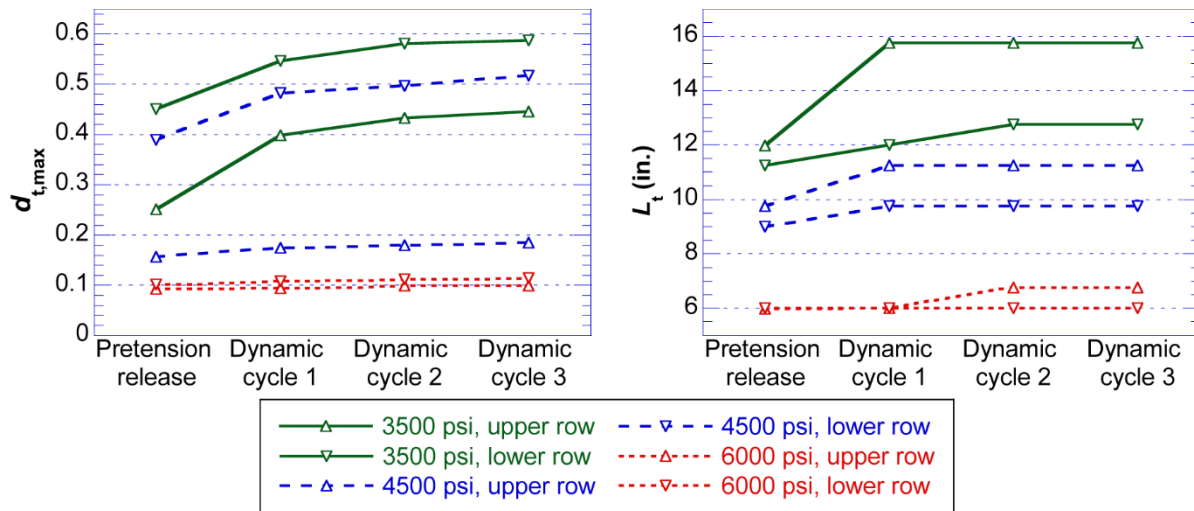
Figure 9. Evolution of $d_{t,max}$ and L_{dt} from static to dynamic simulations with the prestressing strand at all three concrete release strengths.

With Fastener Shoulders

The simplified fastener shoulder models in Figure 4 were employed in additional analyses. For the tie with the prestressing wires, two fastener shoulders embedded in the tie were modeled, and the tie model was quarter symmetric. For the tie with the prestressing strands, a fastener assembly was modeled including two shoulders, two clips, two insulators, one rail pad and the rail, and the model was half symmetric about the center cross-sectional plane. First static FEA of pretension release were conducted for both ties, then for the tie with the prestressing strands, fastener installation was simulated in which the clips were rotated clear of the insulators on top of the rail bases and then released to touch the insulators, resulting in a resultant toe load of 5 kips (22.2 kN).

Figure 10 shows the d_t contours for elements satisfying $d_t≥0.05$ after pretension release without and with the fastener shoulder models for the prestressing wires WG and WH at the 3,500 psi (24.1 MPa) concrete release strength. The minor differences in the damage patterns without and with the fastener shoulders can be mainly attributed to the differences in the FE meshes.

Figure 11 shows the d_t contours for elements satisfying $d_t≥0.05$ after pretension release without and with the fasteners for the prestressing strand SA at all three concrete release strengths. While the damage patterns did not appear to change much in the upper strand plane, they became less connected in the lower strand plane compared to the patterns shown in Figure 7 with no fasteners.

Figure 12 plots the evolution of $d_{t,max}$ for the prestressing wires WG and WH with the 3,500 psi (24.1 MPa) concrete release strength (left) and for the prestressing strand SA at all three concrete release strengths (right) with the fastener shoulders included in modeling. For the prestressing wires WG and WH, the presence of the fastener shoulders did not introduce significant changes in the tensile damages – the minor differences can be attributed mainly to FE meshing. For the prestressing strand SA, the presence of the fastener shoulders appeared to have an effect of redirecting the concrete damages to the upper strand plane, consistent with the upper strand plane, horizontal cracking pattern observed in the field (Figure 1, right). Figure 12 further shows that with the 3,500 psi (24.1 MPa) concrete release strength, $d_{t,max}$ kept increasing under dynamic loading and can conceivably approach 1 (i.e., crack formation) after a sufficiently large number of dynamic loading cycles. Based on the magnitudes of $d_{t,max}$ in these plots, it appeared that a larger number of dynamic loading cycles would be needed for the cracks to develop in concrete ties made with WG than those made with WH or SA, assuming all ties to be produced at the 3,500 psi (24.1 MPa) release strength.
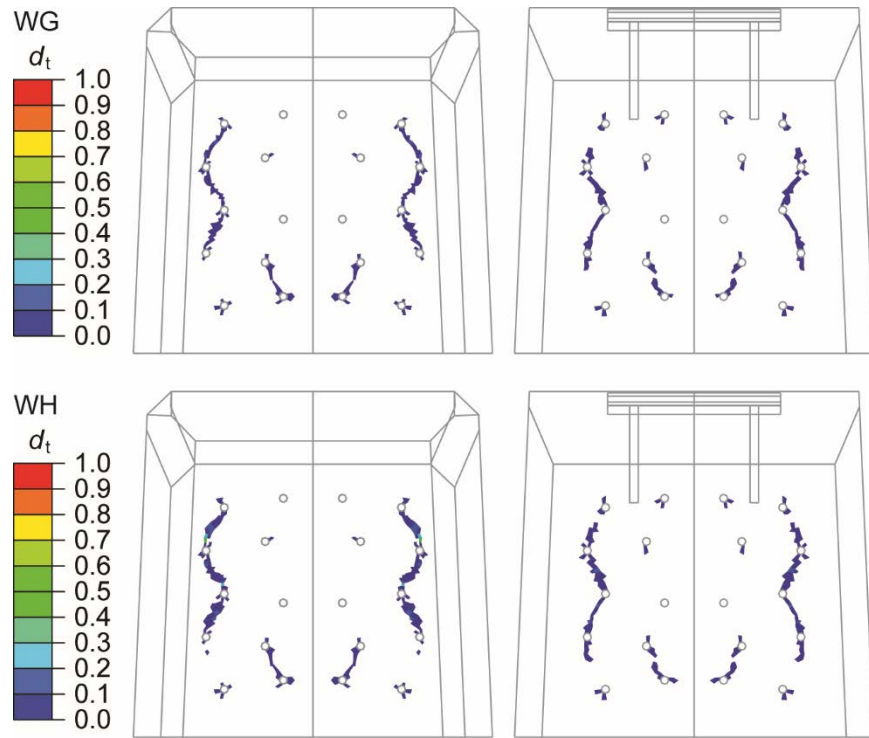
Figure 10. Tensile damage profiles ($d_t{\geq}0.05$) after pretension release without and with the fastener shoulder models for the prestressing wires WG and WH at the 3,500 psi (24.1 MPa) concrete release strength.
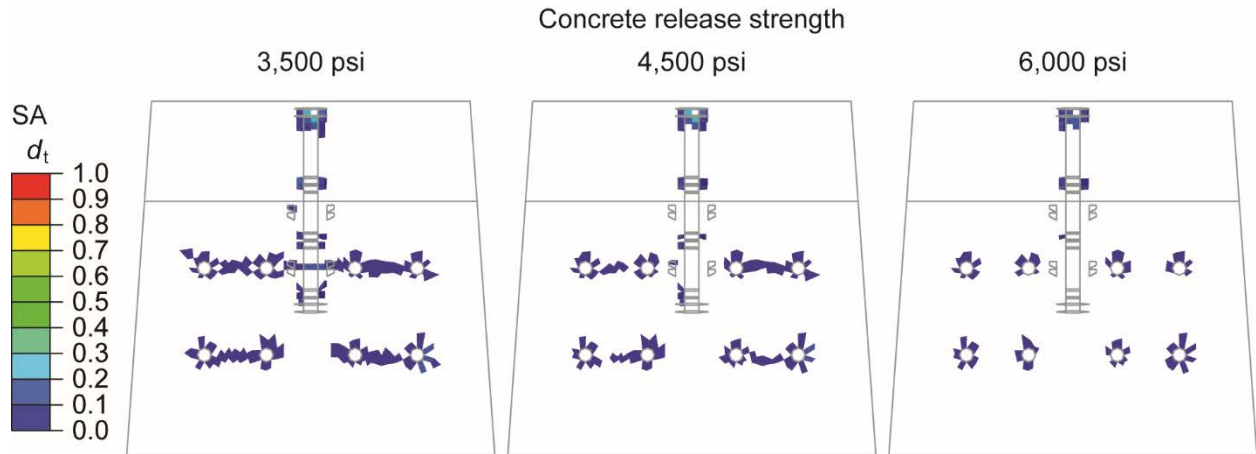
Figure 11. Tensile damage profiles ($d_t{\geq}0.05$) after pretension release with the fastener shoulder models for the prestressing strand SA at all three concrete release strengths.
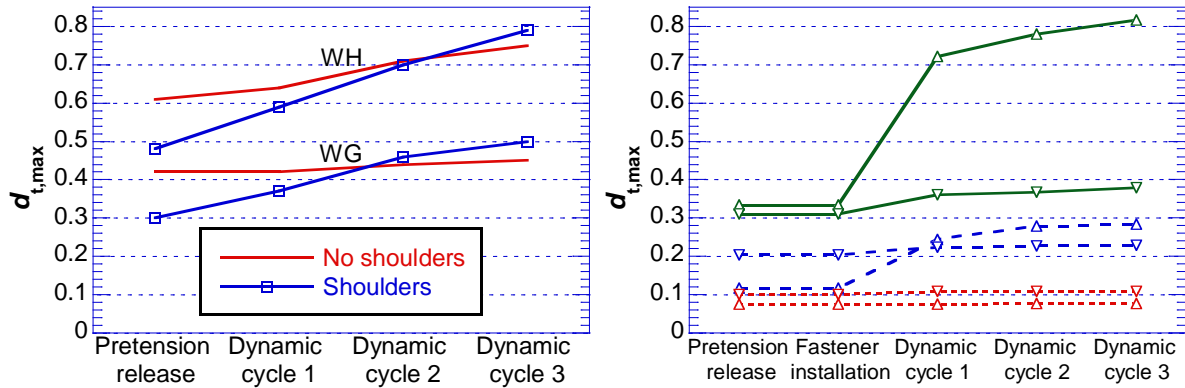
Figure 12. Evolution of $d_{t,max}$ for the prestressing wires WG and WH at the 3,500 psi (24.1 MPa) concrete release strength (left) and for the prestressing strand SA at all three concrete release strengths (right, following the legends of Figure 9) with fastener shoulders included in modeling.

CONCLUSIONS AND RECOMMENDATIONS

An FEA framework incorporating concrete damage and bond modeling for pretensioned concrete crossties was employed to study the causes of concrete bursting/splitting failures. The FEA concluded that concrete release strengths as low as 3,500 psi (24.1 MPa) can lead to initial concrete degradation patterns, upon pretension release during production, for some prestressing wires with certain surface geometries and for a seven-wire prestressing strand. The initial degradation can further develop into macroscopic cracks consistent with field observations after the ties were subjected to dynamic loading cycles. It is recommended that the pretension release phase in concrete tie productions be conducted at sufficiently high concrete release strengths. Alternatively, qualification test standards that subject the concrete crossties to dynamic loading cycles may be developed and implemented to ensure their long term splitting/bursting performances. The two simplified fastener shoulder models included in the study either did not change the failure/cracking pattern (for the wires) or did not change the likelihood of splitting failure (for the strand) at the 3,500 psi (24.1 MPa) concrete strength level.

REFERENCES

1. Hanna, A. N., 1979, "State-of-the-Art Report on Prestressed Concrete Ties for North American Railroads," *PCI Journal*, September-October: 32-61.
2. Yu, H., Jeong, D., Marquis, B., and Coltman, M., 2015, "Railroad Concrete Tie Failure Modes and Research Needs," 2015 Transportation Research Board 94th Annual Meeting, TRB15-0311.
3. NDT Corporation. Assessment of Pulse Velocity Testing to Rate Concrete Cross Tie Conditions. Intermediate progress report submitted to Federal Railroad Administration, 2014.
4. Mayville, R. A., L. Jiang, and M. Sherman. Performance Evaluation of Concrete Railroad Ties on the Northeast Corridor. DOT/FRA/RPD-14/03. Federal Railroad Administration, U.S. Department of Transportation, 2014.
5. Yu, H., and Jeong, D. Y., 2014, "Bond between Smooth Prestressing Wires and Concrete: Finite Element Model and Transfer Length Analysis for Pretensioned Concrete Crossties," Proceedings of the 2014 ASCE Structures Congress.
6. Yu, H., and Jeong, D.Y., 2015, "Finite Element Bond Models for Seven-Wire Prestressing Strands in Concrete Crossties," Proceedings of the 2015 Joint Rail Conference, JRC2015-5758.

7. Yu, H., and Jeong, D.Y., 2016, "Finite Element Bond Modeling for Indented Wires in Pretensioned Concrete Crossties," 2016 Joint Rail Conference, JRC2016-5782.
8. Yu, H., 2017, "A Unified Elastoplastic Bond Model for Prestressing Steel Reinforcements Used in Railroad Concrete Crossties," *in preparation*.
9. Dassault Systèmes, 2012, Abaqus Analysis User's Manual.
10. Arnold, M. L., R. J. Peterman, N. N. B. Bodapati, B. T. Beck, and C. H. J. Wu. "Development of a Standard Bond Test for Indented Prestressing Wires," In Proc. 2013 Joint Rail Conference, JRC2013-2461, 2013.
11. Bodapati, N. N. B., W. Zhao, R. J. Peterman, C. H. J. Wu, B. T. Beck, M. Haynes, and J. R. Holste. "Influence of Indented Wire Geometry and Concrete Parameters on the Transfer Length in Pretensioned Concrete Crossties," In Proc. 2013 Joint Rail Conference, JRC2013-2463, 2013.
12. Bodapati, N. N. B., R. J. Peterman, W. Zhao, B. T. Beck, C. H. J. Wu, J. R. Holste, M. L. Arnold, R. Benteman, and R. Schweiger. "Transfer-Length Measurements on Concrete Railroad Ties Fabricated with 15 Different Prestressing Reinforcements," In Proc. 2013 PCI Convention and National Bridge Conference, 2013.
13. Zhao, W., B. T. Beck, R. J. Peterman, C. H. J. Wu, N. N. B. Bodapati, and G. Lee. "Reliable Transfer Length Assessment for Real-Time Monitoring of Railroad Crosstie Production," In Proc. 2014 Joint Rail Conference, JRC2014-3830, American Society of Mechanical Engineers, 2014.
14. Yu, H., Jeong, D. Y., Choros, J., and Sussmann, T., 2011, "Finite Element Modeling of Prestressed Concrete Crossties with Ballast and Subgrade Support," Proc. ASME 2011 International Design Engineering Technical Conferences & Computers and Information in Engineering Conference, DETC2011-47452.
15. Yu, H., and Jeong, D. Y., 2012, "Railroad Tie Responses to Directly Applied Rail Seat Loading in Ballasted Tracks: A Computational Study," Proc. ASME/ASCE/IEEE 2012 Joint Rail Conference, JRC2012-74149.
16. Arnold, M. L., 2013, Un-Tensioned Pullout Tests to Predict the Bond Quality of Different Prestressing Reinforcements Used in Concrete Railroad Ties. PhD Dissertation, Kansas State University.
17. American Railway Engineering and Maintenance-of-Way Association, 2016, Manual for Railway Engineering, Chapter 30: Ties.

Causes and Prevention of Splitting/Bursting Failure of Concrete Crossties: A Computational Study

Hailing Yu

Mayville, R. A., Jiang, L., and Sherman, M., 2014, "Performance Evaluation of Concrete Railroad Ties on the Northeast Corridor," Report No. DOT/FRA/RPD-14/03, Federal Railroad Administration, U.S. Department of Transportation.
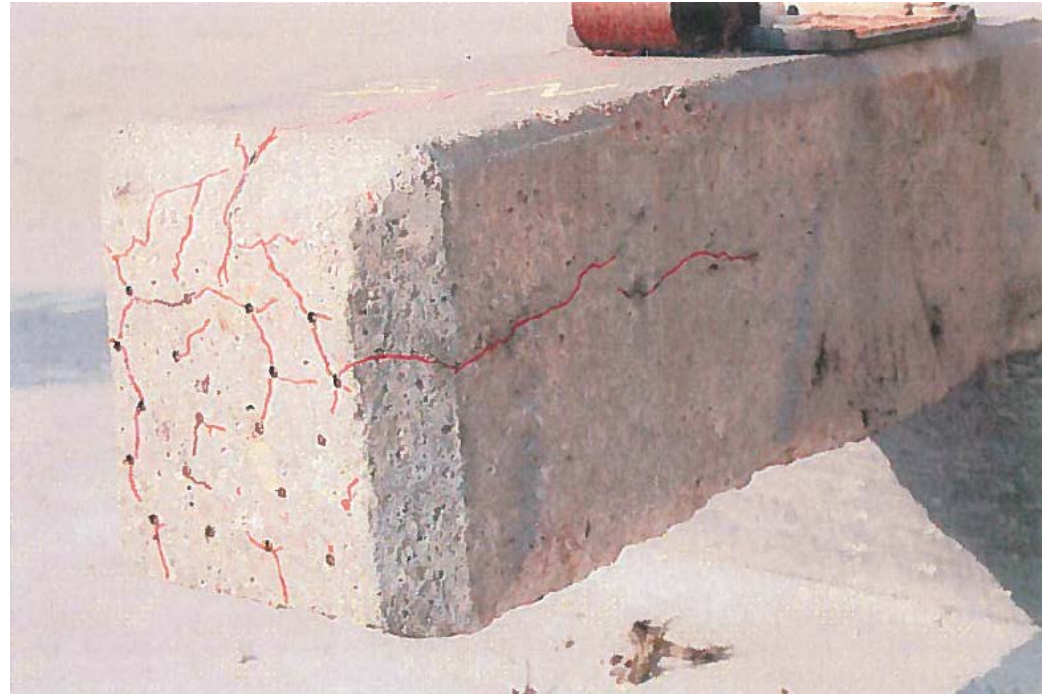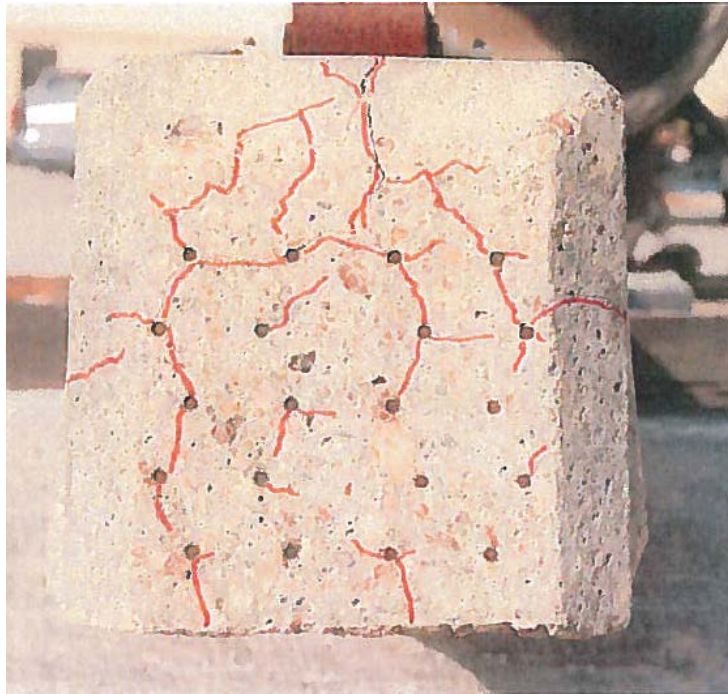
NDT Corporation. Assessment of Pulse Velocity Testing to Rate Concrete Cross Tie Conditions. Intermediate progress report submitted to Federal Railroad Administration, 2014.

Interface Micromechanics
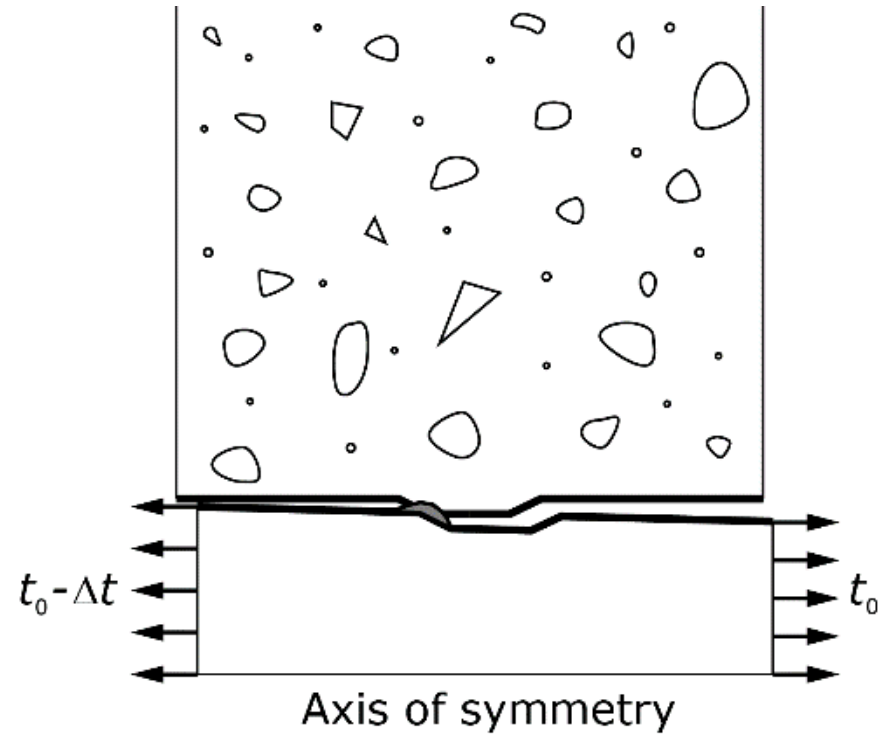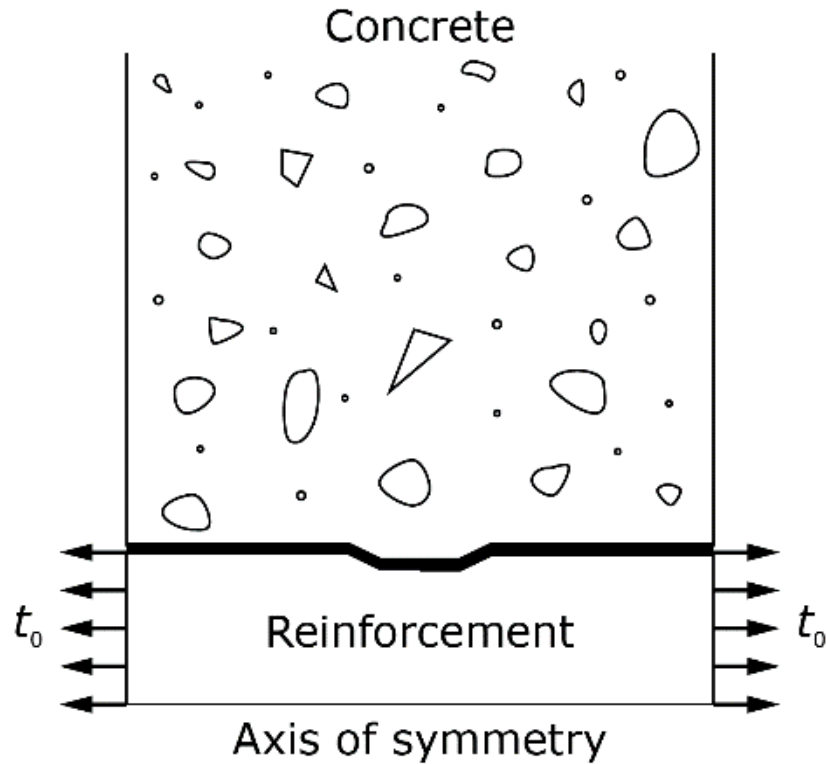
Elastoplastic Bond Model

- Interface stresses

$$\boldsymbol{\sigma} = \sigma\mathbf{n} + \tau_1\mathbf{s} + \tau_2\mathbf{t} \qquad |\tau| = \sqrt{\tau_1^2 + \tau_2^2}$$

- Interface displacements

$$\mathbf{u} = u_\mathrm{n}\mathbf{n} + u_\mathrm{t1}\mathbf{s} + u_\mathrm{t2}\mathbf{t} \qquad \mathbf{u} = \mathbf{u}^\mathrm{el} + \mathbf{u}^\mathrm{pl}$$

- Elasticity

$$\boldsymbol{\sigma} = \mathbf{D}^\mathrm{e}\mathbf{u}^\mathrm{el} = \mathbf{D}^\mathrm{e}\left(\mathbf{u} - \mathbf{u}^\mathrm{pl}\right)$$
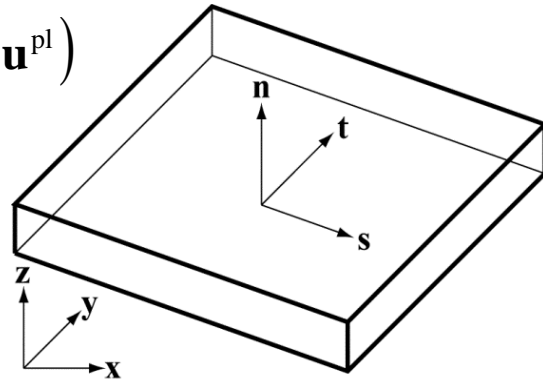
- Yield surface

$$F(\sigma, \tau) = 0$$

- Plastic flow

$$\mathrm{d}\mathbf{u}^\mathrm{pl} = \mathrm{d}\lambda\frac{\partial Q}{\partial\boldsymbol{\sigma}}$$

Yield function	$F = \lvert\tau\rvert + \sigma\tan\phi - a = \lvert\tau\rvert + \mu\sigma - a$
Plastic potential	$Q = \lvert\tau\rvert + \sigma\tan\psi = \lvert\tau\rvert + \mu_{\mathrm{d}}\sigma$
Plastic flow rule	$\mathrm{d}u_{\mathrm{n}}^{\mathrm{pl}} = \mu_{\mathrm{d}}\left\lvert\mathrm{d}u_{\mathrm{t}}^{\mathrm{pl}}\right\rvert \qquad \tau_2\mathrm{d}u_{\mathrm{t1}}^{\mathrm{pl}} = \tau_1\mathrm{d}u_{\mathrm{t2}}^{\mathrm{pl}}$
Bond material constants	$D_{\mathrm{nn}}^{\mathrm{e}} \quad D_{\mathrm{ns}}^{\mathrm{e}}(= D_{\mathrm{nt}}^{\mathrm{e}}) \quad \mu \quad a_0 \quad u_{\mathrm{tc}}^{\mathrm{pl}} \quad \mu_{\mathrm{d}}^{\max} \quad \mu_{\mathrm{dc}} \quad u_{\mathrm{td}}^{\mathrm{pl}}$

Determination of Bond Model Parameters
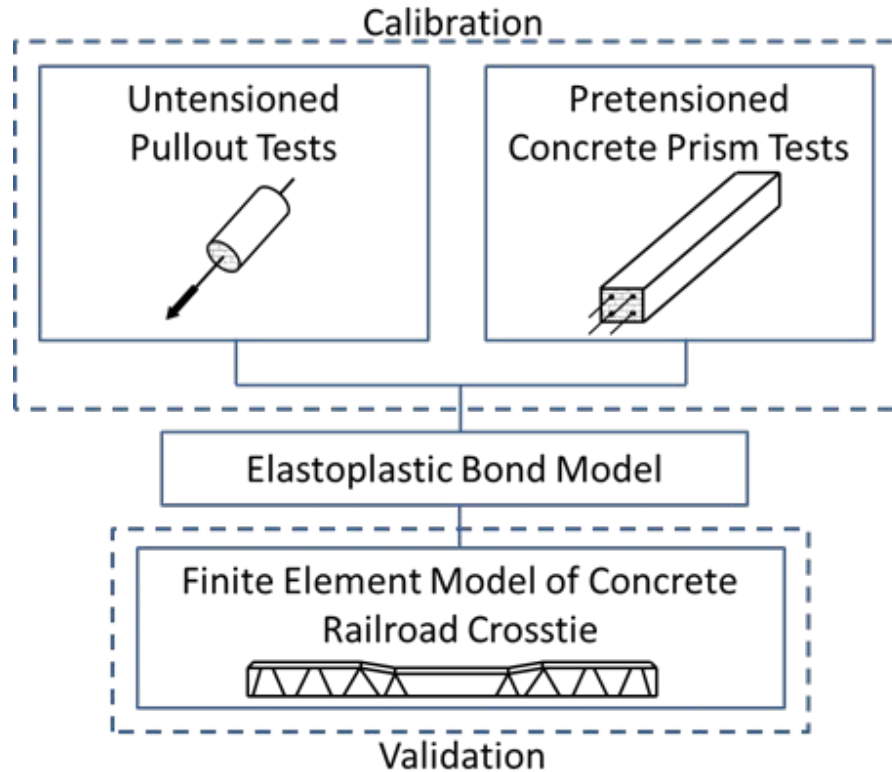
Bond Characteristics from Pullout Tests

Concrete release strength = 6,000 psi

Yield function	$F = |\tau| + \sigma \tan\phi - a = |\tau| + \mu\sigma - a$
Plastic potential	$Q = |\tau| + \sigma \tan\psi = |\tau| + \mu_\mathrm{d}\sigma$
Plastic flow rule	$\mathrm{d}u_\mathrm{n}^\mathrm{pl} = \mu_\mathrm{d}\left|\mathrm{d}u_\mathrm{t}^\mathrm{pl}\right| \qquad \tau_2 \mathrm{d}u_\mathrm{t1}^\mathrm{pl} = \tau_1 \mathrm{d}u_\mathrm{t2}^\mathrm{pl}$
Bond material constants	$D_\mathrm{nn}^\mathrm{e} \quad D_\mathrm{ns}^\mathrm{e}(= D_\mathrm{nt}^\mathrm{e}) \quad \mu \quad a_0 \quad u_\mathrm{tc}^\mathrm{pl} \quad \mu_\mathrm{d}^\mathrm{max} \quad \mu_\mathrm{dc} \quad u_\mathrm{td}^\mathrm{pl}$

Simplified Calibration

Pretensioned Concrete Prism Tests

Elastoplastic Bond Model Parameters
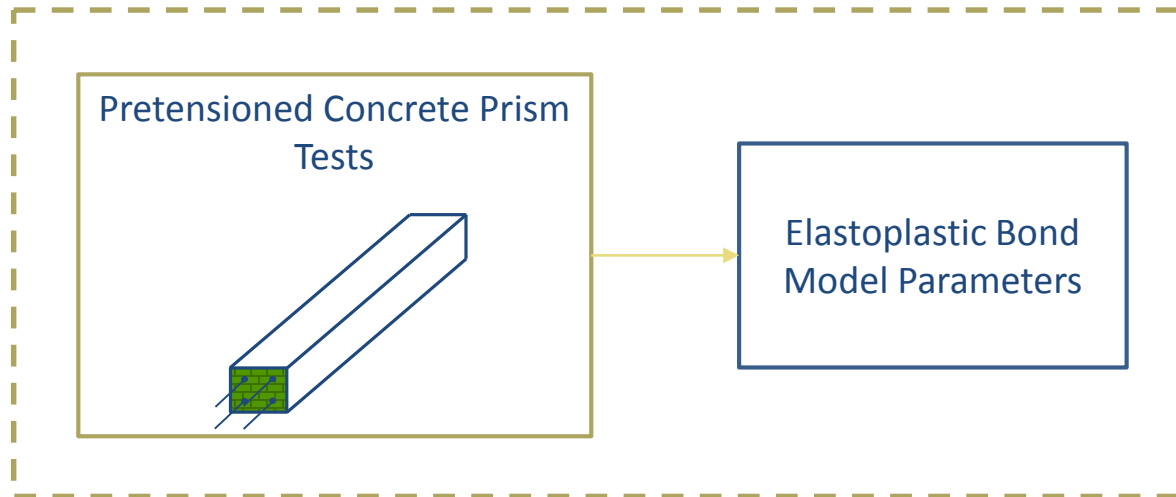
Concrete Tensile Stress-Strain Curve

$d_t=0$: intact material
$d_t>0$: degraded material
$d_t\rightarrow1$: crack formation

Concrete release strength

3,500 psi   4,500 psi   6,000 psi

WG

WH
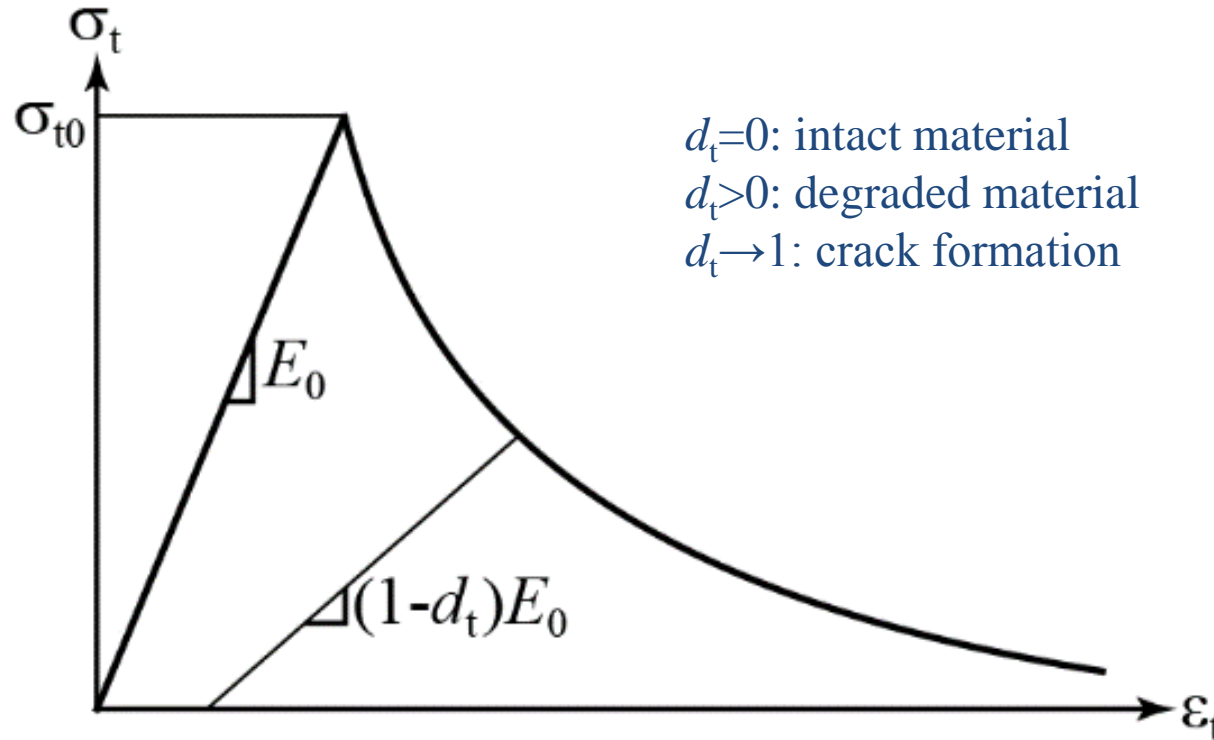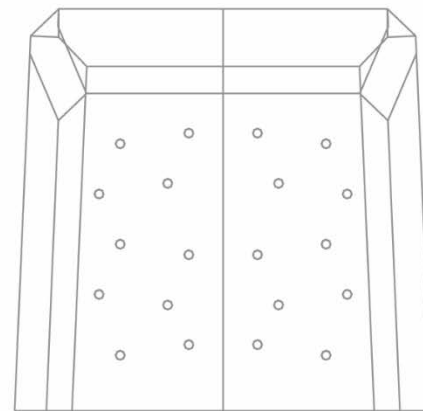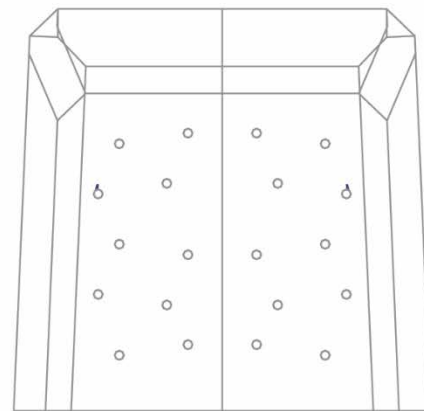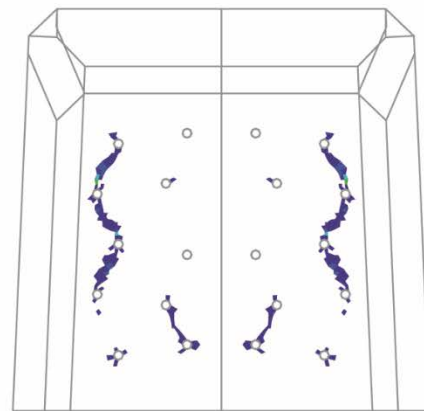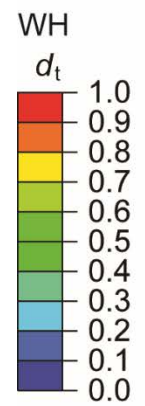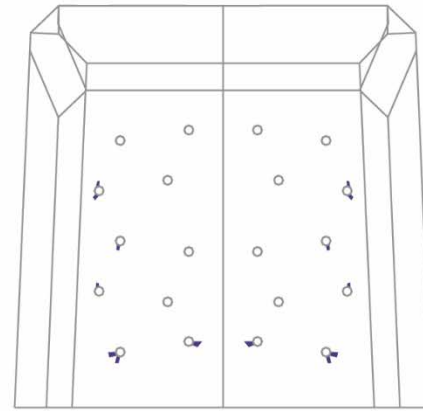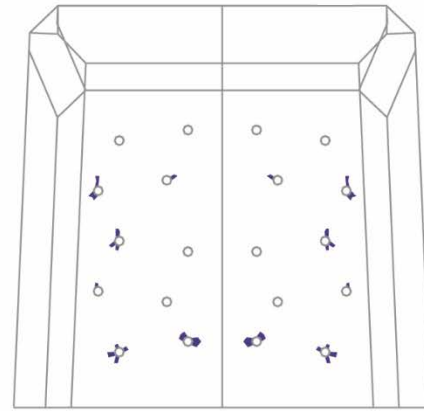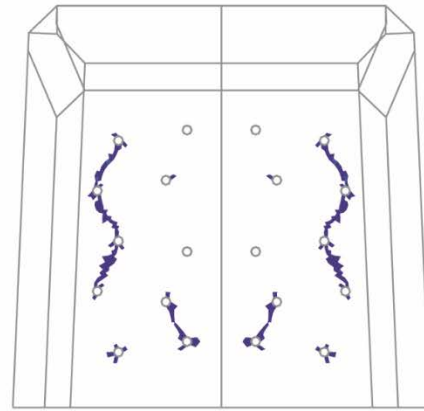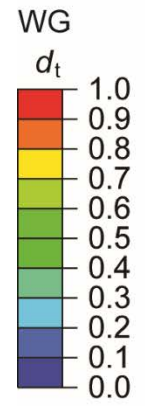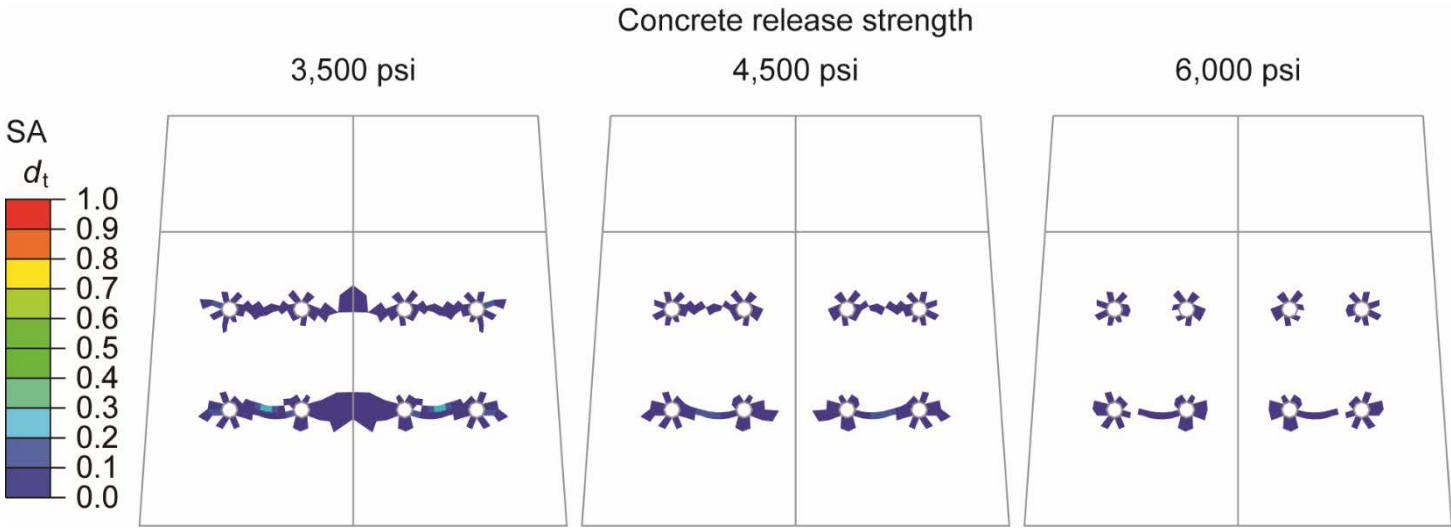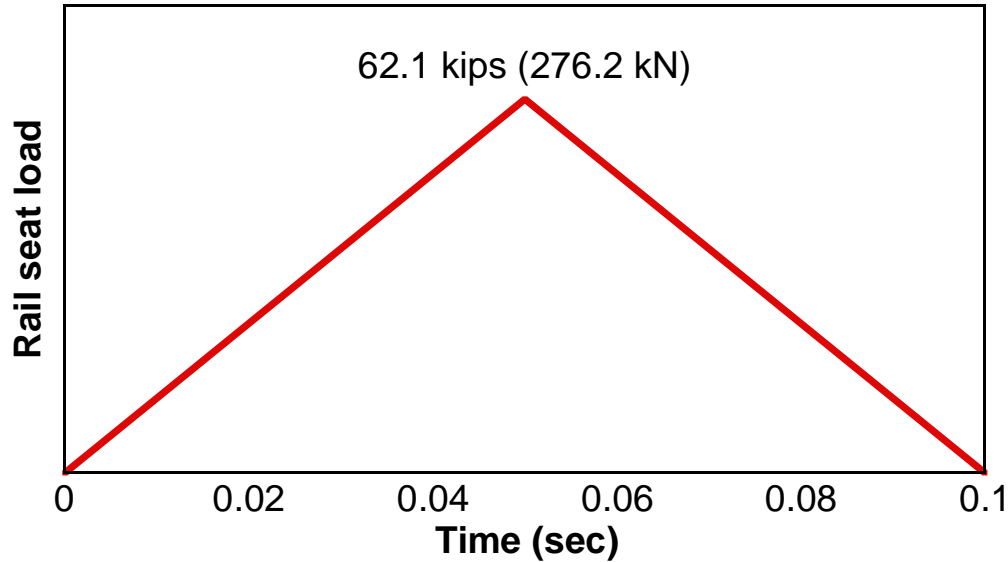
Dynamic load cycles
Axel load: 82 kips
Load distribution factor: 0.505
Impact factor: 200%
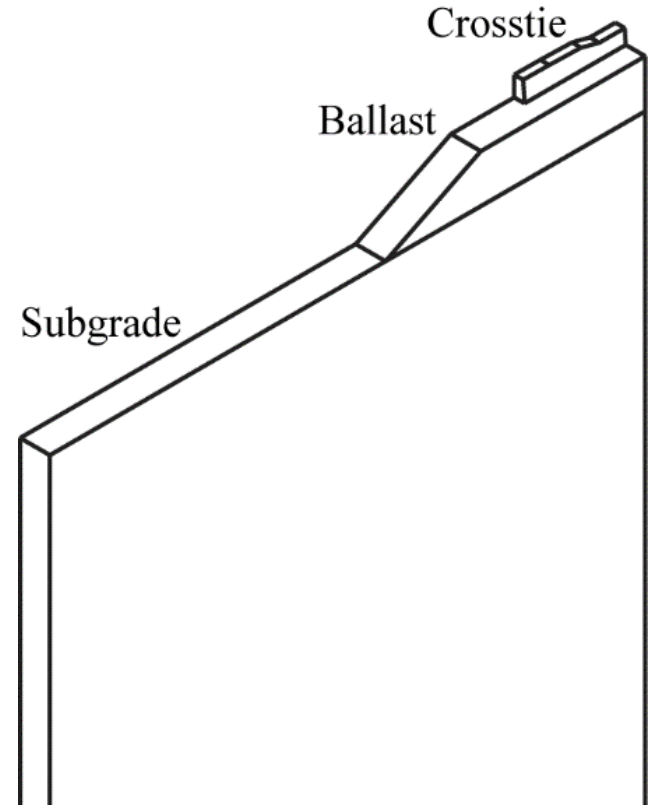
Damage Evolution (Wires)
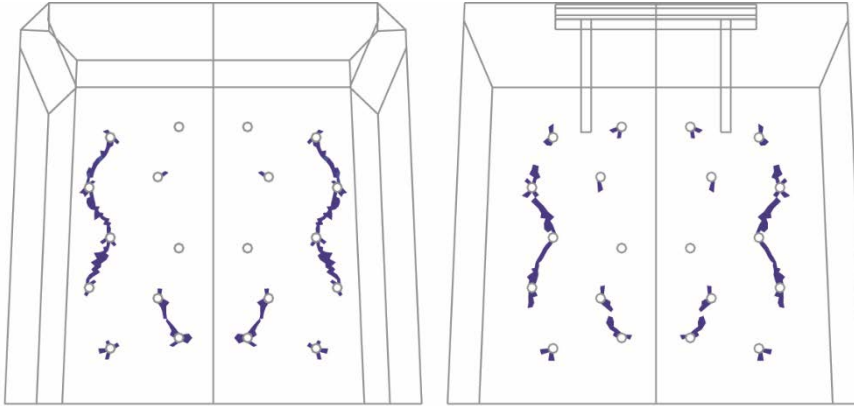
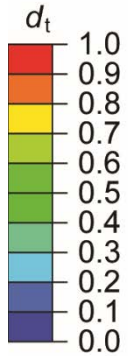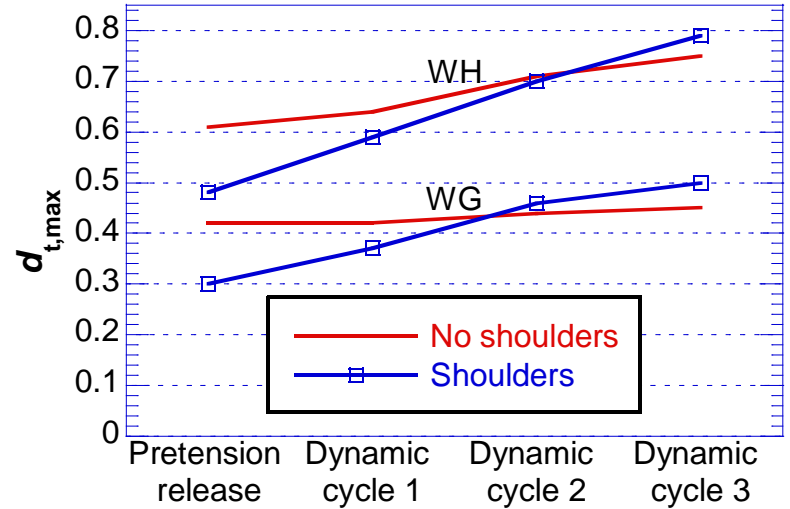**Concrete release strength = 3,500 psi**
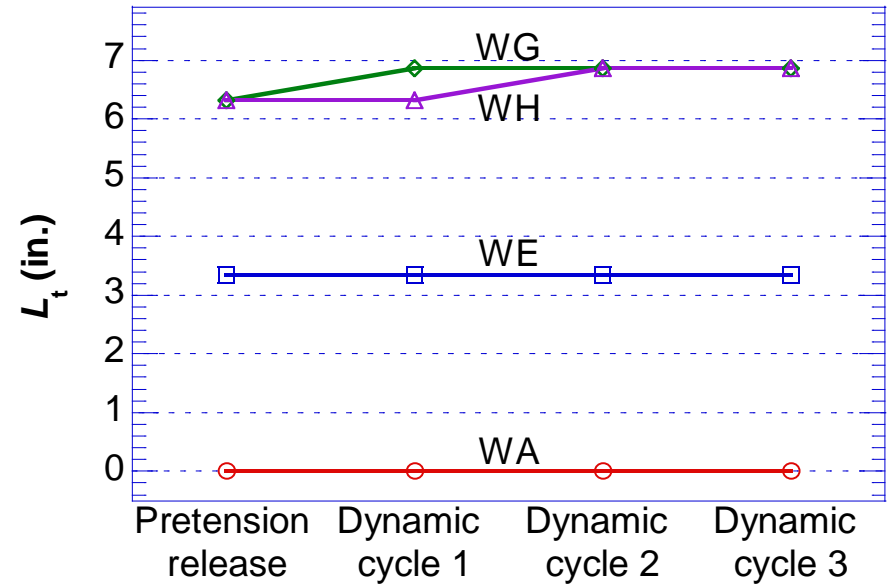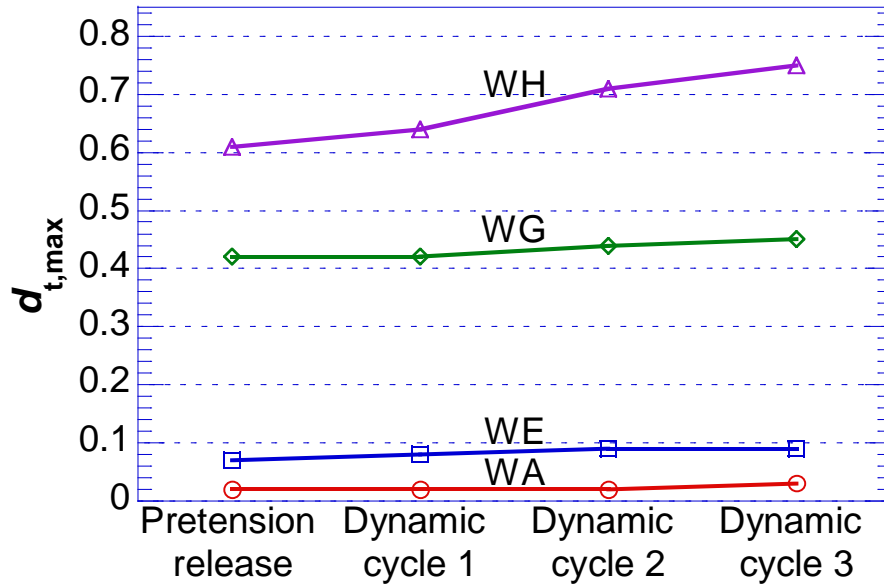
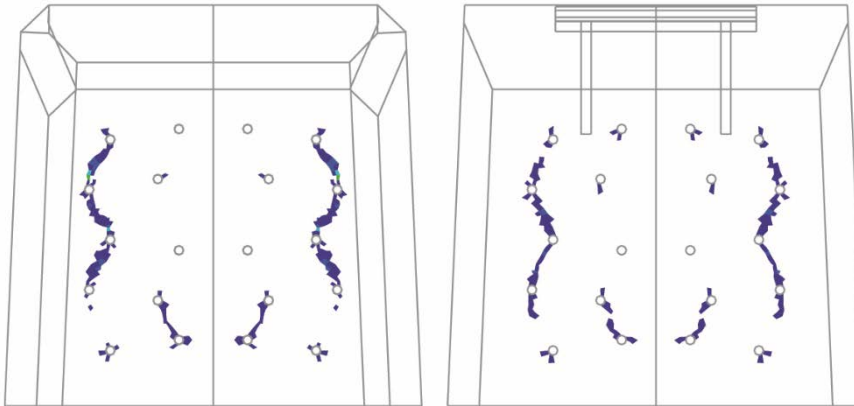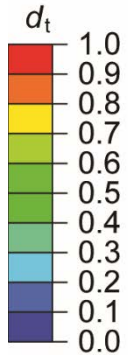# Damage Evolution (Seven-Wire Strand)
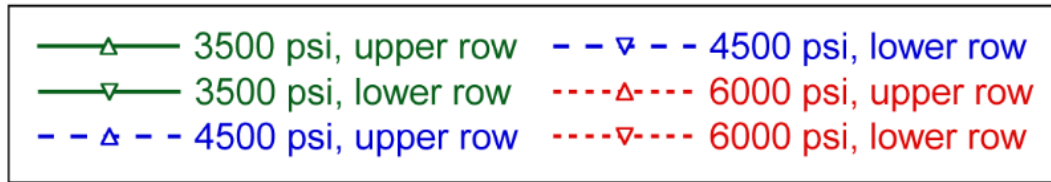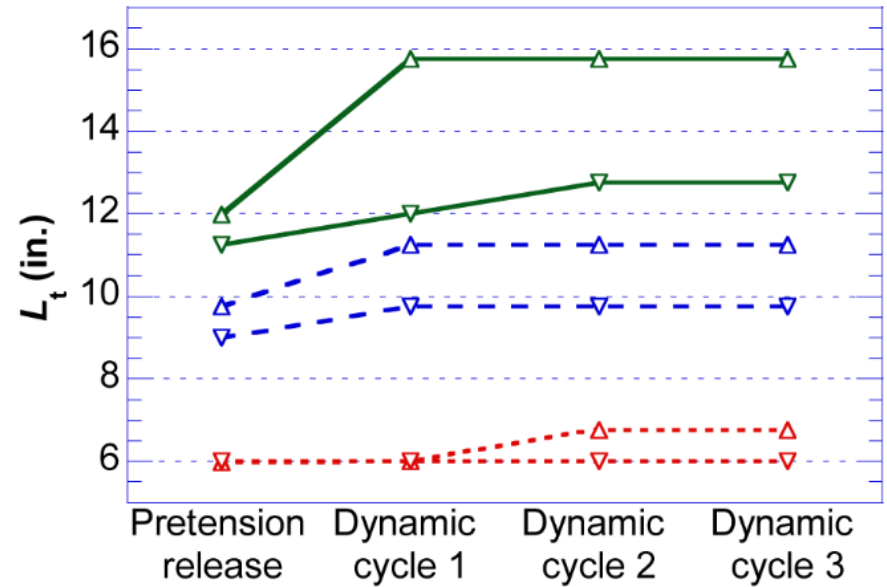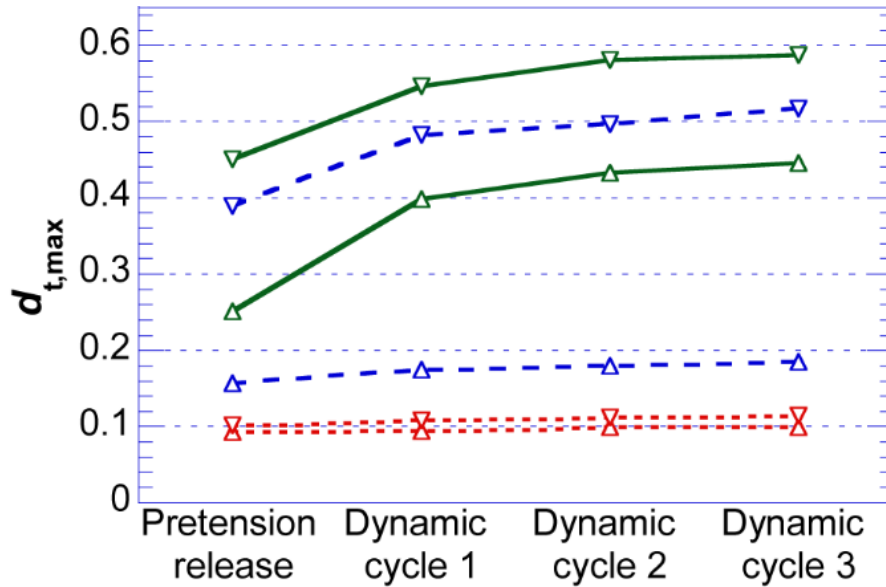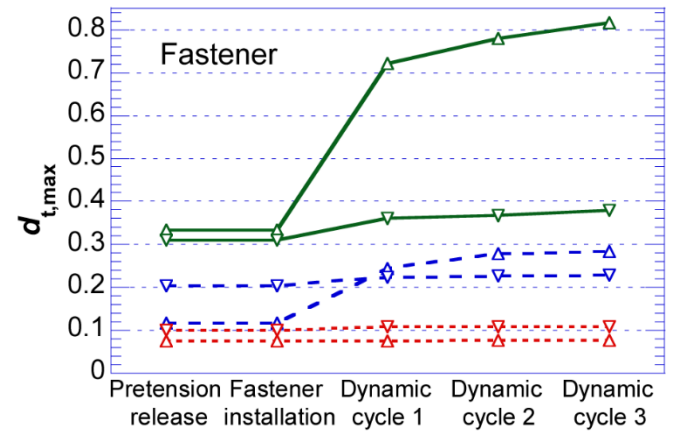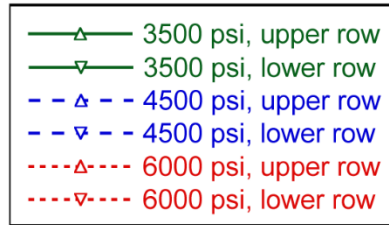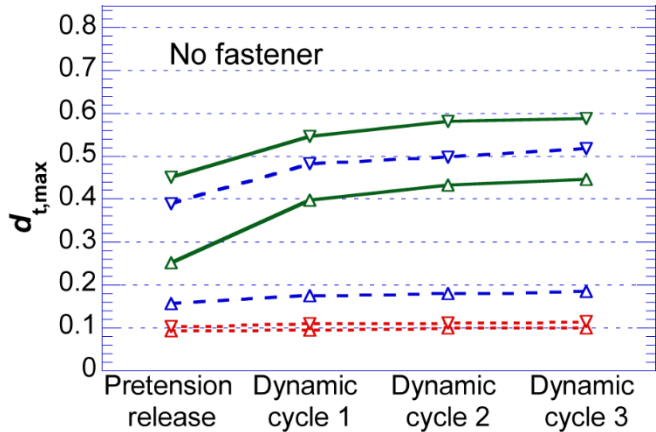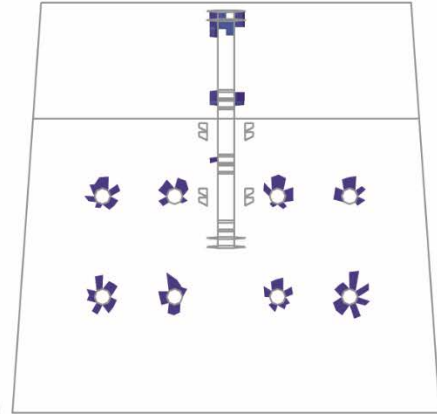
Modeling of Fastener Shoulders
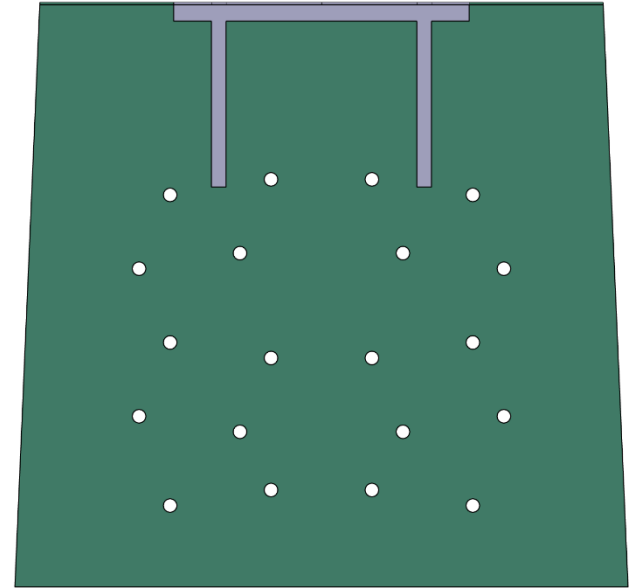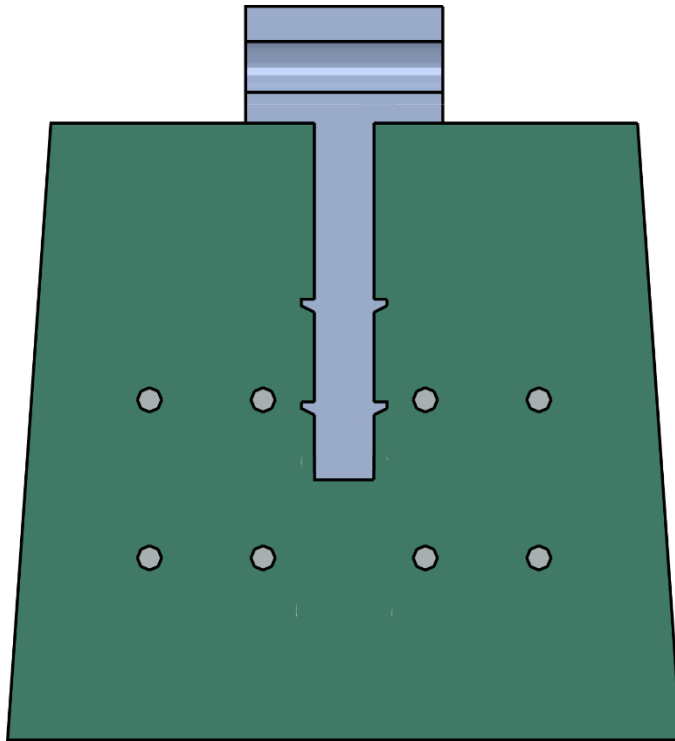
Concrete release strength = 3,500 psi

Concrete release strength

3,500 psi   4,500 psi   6,000 psi

SA d_t

1.0
0.9
0.8
0.7
0.6
0.5
0.4
0.3
0.2
0.1
0.0

No fastener

3500 psi, upper row
3500 psi, lower row
4500 psi, upper row
4500 psi, lower row
6000 psi, upper row
6000 psi, lower row

Fastener

Pretension release   Dynamic cycle 1   Dynamic cycle 2   Dynamic cycle 3

Pretension release   Fastener installation   Dynamic cycle 1   Dynamic cycle 2   Dynamic cycle 3
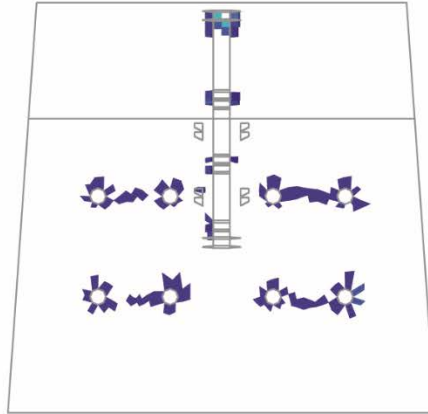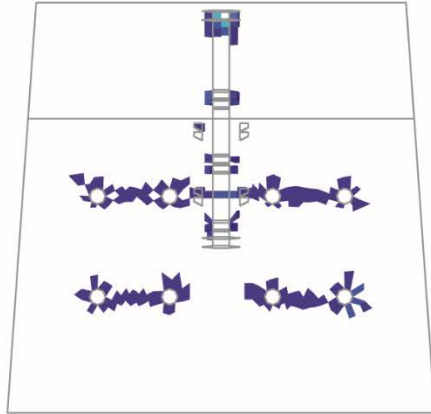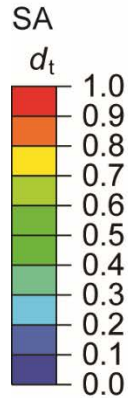
Conclusions

- Low concrete release strengths can lead to initial concrete degradations during prestress transfer in production, for prestressing wires with certain surface geometries and the seven-wire strand;
- Subjected to dynamic loading cycles, initial concrete degradations can develop into macroscopic bursting/splitting cracks;
- The presence of fastener shoulders does not change the concrete degradation patterns (for the wires) or the likelihood of splitting failure (for the seven-wire strand) at the 3,500 psi concrete strength level;
- The elastoplastic bond model is key to differentiating the interface bond-slip and dilatational effects and predicting the splitting/bursting failures.

Recommendations

- Conduct the pretension release phase during concrete tie productions at sufficiently high concrete release strengths.

- Develop and implement qualification test standards that incorporate dynamic loading cycles to ensure long term splitting/bursting performances.

Acknowledgements

- The Office of Research, Development and Technology, Federal Railroad Administration, U.S. Department of Transportation sponsored this study.

- Messrs. Gary Carr and Cameron Stuart of the Track Research Division provided directions to this study.